ELSEVIER

Seminars in
NUCLEAR
MEDICINE

Radiopharmaceuticals for Renal Positron Emission Tomography Imaging

Zsolt Szabo, MD, PhD, Jinsong Xia, MD, PhD, and William B. Mathews, PhD

Radiopharmaceuticals for functional renal imaging, including renal blood flow, renal blood volume, glomerular excretion, and metabolism have been available for some time. This review outlines radiopharmaceuticals for functional renal imaging as well as those that target pertinent molecular constituents of renal injury and repair. The angiotensin and endothelin receptors are particularly appealing molecular targets for renal imaging because of their association with renal physiology and pathology. Other targets such as the vascular endothelial growth factor (VEGF) receptor, integrin, or phosphatidylserine have been investigated at length for cancer imaging, but they are just as important constituents of the renal injury/repair process. Various diseases can involve identical mechanisms, such as angiogenesis and apoptosis, and radiopharmaceuticals developed for these processes in other organs can also be used for renal imaging. The sensitivity and spatial resolution of positron emission tomography makes it an ideal tool for molecular and functional kidney imaging. Radiopharmaceutical development for the kidneys must focus on achieving high target selectivity and binding affinity, stability and slow metabolism in vivo, and minimal nonspecific accumulation and urinary excretion.
Semin Nucl Med 38:20-31

Molecular Mechanisms of Renal Injury

A critical challenge to diagnostic imaging is to find imaging biomarkers with high sensitivity and quantitative accuracy for kidney injury and a capacity to document tissue repair or deterioration in a timely fashion. Positron emission tomography (PET) is the ideal molecular imaging technology because of its high spatial resolution, sensitivity, and quantitative accuracy; however, at present, the availability of radiopharmaceuticals is limited.

Acute Injury

Acute renal injury can be initiated by organ hypoperfusion, radiation exposure, nephrotoxic drugs, infection, or sepsis. The functional consequences of acute injury-reduced blood flow, reduced glomerular filtration, and reduced tubular function are secondary events; primary response to injury occurs at the molecular level. It is the cascade of such molecular events that precedes irreparable damage and hence needs to be targeted therapeutically to prevent, alleviate, or reverse impairment. Molecular imaging is important because it can offer insight into the biology of injury and provide guidance toward early implementation of a specific, effective therapeutic strategy.

Omnipresent in tissue injury is intracellular accumulation of free calcium and oxidative radicals that activate cell response routes and repair mechanisms. The c-Jun N-terminal kinase and the p38 protein can reduce the deleterious effects of reperfusion injury. Drugs that can affect these proteins are monoamino oxidase inhibitors[1] and specific antisense oligonucleotides.[2] Both classes of drugs have been radiolabeled for PET.[2,3] Ultimately, the balance between protein kinases and protein phosphatases will determine the biological outcome: cell survival or cell death.[4] The group of signaling kinases such as the extracellular signal-regulated kinases and the protein kinase B mediate tissue survival. Activation of these proteins involves oxidative stress, the epidermal growth factor and the insulin-like growth factor 1 (IGF-1).

The peptic nucleic acid (PNA) chimera ^{64}Cu-SBTG$_2$-*KRAS* is a novel class radiopharmaceutical designed for specific targeting of the IGF-1 receptor (Fig. 1).[5] The peptide com-

Russell H. Morgan Department of Radiology and Radiological Sciences, Division of Nuclear Medicine, Johns Hopkins University School of Medicine, Baltimore, MD.

The research related to this publication has been supported by NIH grants DK-50,183 and CA-115532 and by a grant from the Center for Biological Modulators/KRICT Korea.

Address reprint requests to Zsolt Szabo, MD, PhD, Russell H. Morgan Department of Radiology and Radiological Sciences, Division of Nuclear Medicine, The Johns Hopkins Medical Institutions, 601 N Caroline St, Room # JHOC 3233, Baltimore, MD 21287. E-mail: zszabo@jhmi.edu

0001-2998/08/$-see front matter
doi:10.1053/j.semnuclmed.2007.09.008

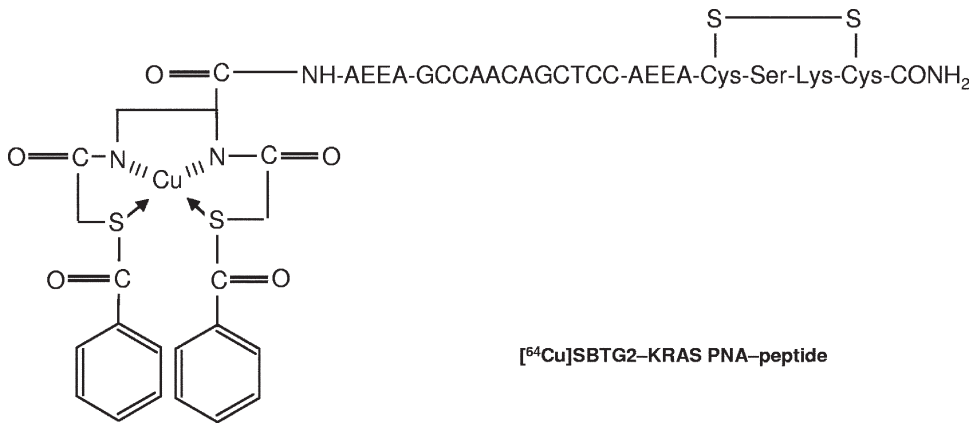

Figure 1 ^{64}Cu-SBTG$_2$-*KRAS* PNA–peptide chimera.[5]

ponent of the chimera is responsible for receptor binding and internalization of the construct that will permit delivery of an oligonucleotide probe to its target mRNA for diagnostic or therapeutic purposes. Another PNA specific for the MYC[a] mRNA that binds to the IGF-1 receptor has been radiolabeled with ^{99m}Tc and demonstrated significant accumulation in the kidneys.[6] This approach may represent a new way to image survival signaling in the kidney. Other important response molecules of acute renal injury are the focal adhesion kinase, the heat shock proteins,[7] and the glucose-regulated proteins.[4]

Chronic Injury

Cyclosporine A nephrotoxicity is a classic example of chronic kidney injury. Acutely, cyclosporine A causes arteriolar vasoconstriction and reduced renal blood flow, changes that are readily detected by functional imaging. Early detection of injury will require the development of radiopharmaceuticals for response molecules of chronic injury. Interesting targets are components of the endothelin and angiotensin signaling systems. Chronic cyclosporine A nephrotoxicity involves activation of the renin angiotensin system, release of endothelin-1, and dysregulation of nitric oxide synthase (NOS), changes that result in reduced blood flow and the glomerular filtration rate (GFR). Hypoxia leads to accumulation of reactive oxygen species, upregulation of transforming growth factor beta 1 (TGFb1), apoptosis and inflammation. Activation of the renin angiotensin system also induces renal injury by both hemodynamic and nonhemodynamic mechanisms. Osteopontin also represents a very interesting imaging target due to its dramatic upregulation in cyclosporine nephropathy.[8] Chronic overexposure to cyclosporine A results in apoptosis which involves activation of angiotensin II, nitrous oxide, TGF-b1, EGF, caspases, and p53.

Tubuloglomerular Feedback

One of the fundamental regulatory mechanisms in the kidney is coordination of tubular function and glomerular filtration. The purpose of this coordination is to prevent excessive fluctuations in total body salt and water content in response to changes of the GFR.[9] Glomerulotubular balance depends on both GFR and the activity of the tubuloglomerular feedback mechanism. The sensor of this signaling system is in the macula densa and its responsive elements are the angiotensin receptors, the contractile glomerular mesangium and glomerular arterioles.[10] In normotensive animals, nitric oxide (NO) counteracts angiotensin II mediated vasoconstriction in both pre- and postglomerular microcirculation.[11]

Increased secretion of angiotensin II in renovascular hypertension enhances tubuloglomerular feedback responsiveness and leads to retention of sodium and volume dependent hypertension. Circulating components of the renin angiotensin system are less affected than its components at the organ-tissue level, and patients with renovascular hypertension may have normal plasma renin and angiotensin II. Both intrarenal and extrarenal events in arterial hypertension are attenuated by therapeutic blockade of the renin angiotensin system,[12] therefore, making the angiotensin AT1 receptor subtype an appealing target for imaging renal disease.

Reduced renal perfusion in renovascular hypertension activates the local formation of angiotensin II, which results in vasoconstriction (a short-term pharmacological effect), and remodeling (long-term regulatory effect) of afferent and efferent arterioles.[13] The effect on efferent resistance is hemodynamically more important[14] because of the smaller luminal dimension of the efferent arteriole.[15] This difference in response to angiotensin II is utilized in captopril renography.

Angiogenesis

Angiogenesis is a strong candidate for molecular imaging of renovascular nephropathy, diabetic nephropathy, and renal cell cancer. Hypoxia will result in induction of the transcription of hypoxia-inducible factor (HIF-1) and upregulation of VEGF signaling. This upregulation plays a role in mitogenic, antiapoptotic, and vascular permeability effects of the VEGF that is released by ischemic tubular epithelial cells. In the kidneys, VEGF receptor proteins are localized to the endothelium of blood vessels.[16] Favorable biological response to

[a]MYC is a transcription factor upregulated in renal tissue injury that is involved in the control of cell proliferation and its balance with cell apoptosis.

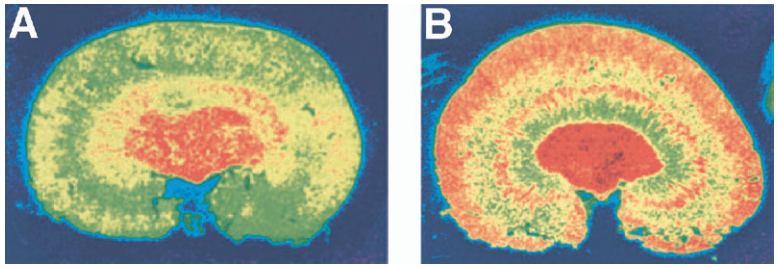

Figure 2 ^{125}I-VEGF binding in the kidney from control (A) and diabetic (B) rats.[21] (Copyright © 1999 American Diabetes Association. From Diabetes 48:2229-2239, 1999. Reprinted with permission from *The American Diabetes Association*.) (Color version of figure is available online.)

VEGF release involves both stimulation of capillary supply and promotion of tubular cell repair.[17]

VEGF is upregulated in clear-cell renal cell carcinoma as a result of loss of the von Hippel Lundau tumor suppressor gene and activation of the hypoxia response pathway.[18] Two targeted agents, an antibody against VEGF (bevacizumab) and an epidermal growth factor receptor tyrosine kinase inhibitor (erlotinib), have been investigated in the treatment of metastatic clear-cell renal carcinoma. These treatments have resulted in significant increases in progression-free survival rates compared with other forms of treatment.[19] Bevacizumab has been radiolabeled with both indium-111 for SPECT imaging and zirconium-89 for PET. Zirconium-89 is a cyclotron produced positron emitter with a half-life of 3.27 days, which permits prolonged imaging of tumors up to 168 hours after injection.[20] Accumulation of monoclonal antibodies in the kidneys may be hampered by their large size, although a direct contact with surface expressed binding sites should be possible.

A typical microvascular disease of the kidneys with upregulation of the VEGFR-2 receptor subtype is diabetic nephropathy (Fig. 2). VEGFR-2 is the most important receptor responsible for initiation of signal transduction pathways and the biological actions of VEGF.[21] ^{64}Cu-DOTA-VEGF$_{121}$ has been used for imaging experimental animals. Although variance in kidney uptake of the radiopharmaceutical was significant, successful partial blocking of kidney uptake with a limited dose of VEGF$_{121}$ demonstrated the specificity of the radiopharmaceutical for the VEGFR receptor in vivo.[22]

Several modes of counteracting VEGF have proven effective in animal models including the use of antisense oligonucleotides, administration of VEGF-neutralizing antibodies, the use of a soluble VEGF receptor chimeric protein, and the inhibition of VEGF signaling using specific kinase inhibitors.[23,24] Unfortunately anti-VEGF therapy has many side effects, including those that affect the kidneys, specifically proteinuria and hypertension[25]; thus, the proper selection of patients for therapy by imaging of VEGF or VEGFR is of great importance. One alternative way is to modulate VEGF via the renin angiotensin system. Because angiotensin II potentiates VEGF-induced angiogenesis,[26] this effect can be reduced by blockade of the renin-angiotensin system.[27]

VG76e, a monoclonal antibody that recognizes certain isoforms of human VEGF, has been labeled with iodine-125 for gamma and iodine-124 for PET imaging. Three iodination strategies have been evaluated: direct labeling using the IodoGen method, indirect labeling with the Bolton-Hunter method, and indirect labeling with the approach of Zalutsky and coworkers.[28] Direct iodination resulted in loss of immunoreactivity, likely the result of an overabundance of iodine binding tyrosine in the complementary regions resulting in hyperiodination and loss of function. Immunoreactivity was preserved with the indirect labeling methods.

Through alternative splicing of RNA, VEGF may exist as at least 7 different molecular isoforms, having 121, 145, 148, 165, 183, 189, or 206 amino acids. VEGF$_{121}$ has been conjugated with 1,4,7,10-tetraazacyclododecane-*N*,*N*′,*N*″,*N*‴-tetraacetic acid (DOTA) and radiolabeled with copper-64 as ^{64}Cu-DOTA-VEGF$_{121}$. Tumor-bearing mice demonstrated high binding of this radiopharmaceutical to the tumor as well as other organs, notably the kidney. Because it was not cleared by the kidneys, accumulation was likely an indication of specific binding to the VEGFR. Specific binding was demonstrated in animals treated with unlabeled VEGF$_{121}$.[22] Although imaging of the VEGFR in renal diseases has yet to be reported, other noncancer applications have been investigated including imaging the upregulation of the VEGFR in experimental myocardial infarction and models of limb ischemia.[29]

Other attractive targets for diagnostic imaging and therapy are integrins. Integrins are extracellular matrix proteins involved in cellular adhesion and angiogenesis. The most studied integrin is $\alpha_v\beta_3$. Cyclic Arg-Gly-Asp (RGD) containing peptides are $\alpha_v\beta_3$ antagonists that can be radiolabeled with the positron-emitting radioisotopes fluorine-18 or copper-64.[30] Integrin targeting is a novel approach to the treatment of renal graft rejection. The $\alpha_v\beta_3$ integrin is upregulated in tubular epithelial cells and peritubular capillaries of rat allografts as well as the perivascular cellular infiltrates of allografts and correlates with signs of vascular or tubulointerstitial rejection. In animal models administration of an integrin antagonist reduced the histological signs of acute rejection, the intensity of the mononuclear cell infiltration, and cell proliferation in the grafted kidneys. The fluorine-18 labeled RGD peptide (Fig. 3) that binds to $\alpha_v\beta_3$ expressing tumors has been tested in both animals[31] and human subjects.[32]

The RGD peptide c(RGDyK) has also been labeled with copper-64 via coupling with DOTA. Introduction of a bi-

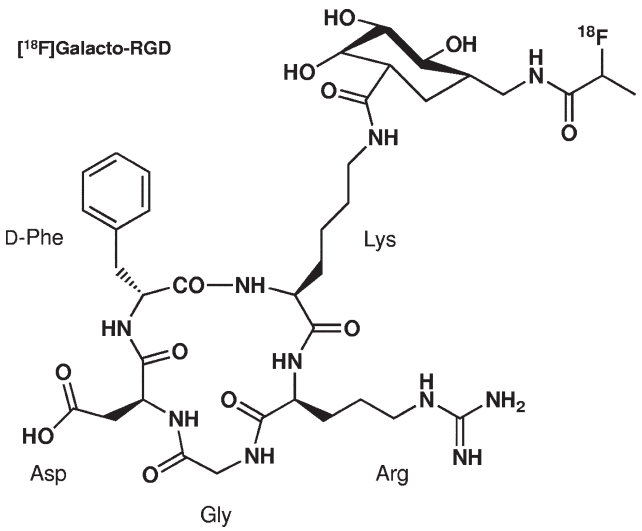

Figure 3 Structure of ^{18}F-Galacto-RGD.[31]

functional poly(ethylene glycol) or PEG between the peptide and DOTA to form ^{64}Cu-DOTA-PEG-RGD significantly improved in vivo kinetics. Further improvement was achieved by using a dimeric RGD peptide which resulted in ^{64}Cu-DOTA-PEG-E[c(RGDyK)]$_2$ (Fig. 4) This radiopharmaceutical demonstrated strong and displaceable binding to cancer cells expressing the $\alpha_v\beta_3$ receptor.[33] Other agents of angiogenesis that could be tested for renal imaging are fluorine-18 labeled RGF containing glycopeptide,[31] ^{99m}Tc EC endostatin,[34] iodine-123 angiostatin,[35] and ^{18}F-fluoropropylsqualamine.[36]

Apoptosis

Interstitial fibrosis and tubular atrophy are hallmarks of chronic renal injury. Although the pathogenesis of tubular atrophy is poorly understood, apoptosis apparently plays a greater role than necrosis. Examples of diseases with pronounced renal epithelial apopotosis include polycystic renal disease, glomerulonephritis, glomerulosclerosis, lupus nephritis and transplant rejection[37] as well as radiation induced nephritis.[38] Of particular interest in nuclear medicine is radiation injury of the kidneys from radiopeptide therapy. Documentation of damage by molecular imaging has a potential for patients treated with radiopeptides or external radiation.

Annexin V is a 36-kDa calcium-dependent phospholipid binding protein with high affinity for the membrane phospholipid phosphatidylserine (PS). Annexin V can detect extracellular PS exposure that is the hallmark of apoptosis. F-18 annexin V is a recently introduced apoptosis imaging agent with much lower accumulation in normal kidneys than ^{99m}Tc-annexin V.[39] Annexin V has also been radiolabeled with the positron emitter I-124.[40] Annexin V as a large molecule may accumulate in glomerular endothelial injury but may not reach the tubular cells to detect apoptosis in the kidneys. Better candidates for renal imaging are smaller peptides such as $Tat_{49\text{-}57}$-yDEVDG-NH_2 and Tat_{57}–49-yDEVDG-NH_2 that show accumulation in apoptotic cells.[41]

The biotin-avidin method has also been applied to apoptosis imaging. This involves a 3-step technique. First, apoptotic cells are pretargeted with biotinylated annexin V, followed by an avidin chase to eliminate free biotinylated products. Subsequently copper-64-labeled streptavidin is administered and binds to the biotin annexin complex with high affinity.[42]

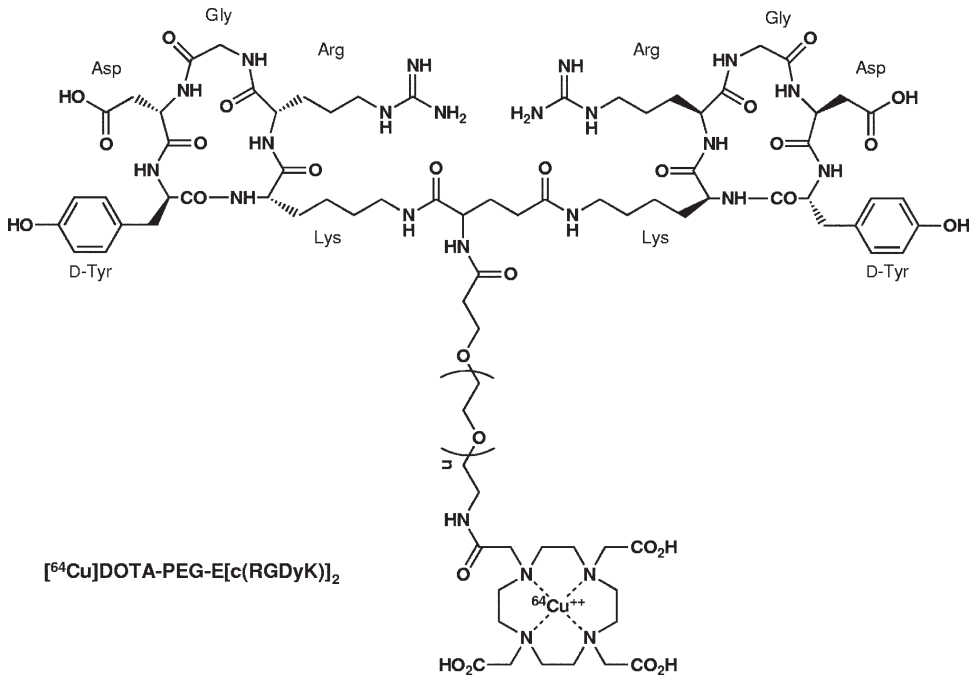

Figure 4 Structure of ^{64}Cu-DOTA-PEG-E[c(RGDyK)]$_2$.[33]

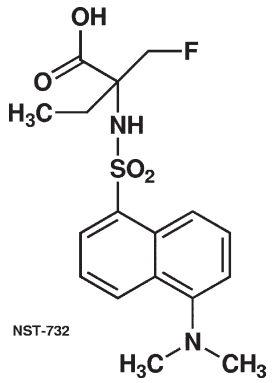

Figure 5 Structure of NST-732.[43]

NST-732 (Fig. 5) is a low-molecular weight apoptosis marker and a member of the so-called ApoSense family of substances. This molecule contains a fluorophore for fluorescent detection and could potentially be labeled with ^{18}F for PET imaging. In a rat renal ischemia/reperfusion injury model that was based on 45 minutes of renal artery clamping, NST-732 fluorescent microscopy detected apoptosis in the ischemic kidney but not the healthy kidney after IV administration (Fig. 6). NST-732 accumulation correlated with terminal deoxynucleotidyl transferase-mediated dUTP nick end labeling (TUNEL) staining for apoptosis, with caspase activation and with a disruption of mitochondrial membrane potential.[43]

Amyloidosis

Amyloidosis is a systemic disease with extracellular deposition of insoluble fibrils. Involvement of the kidney is frequent and progresses to end-stage renal disease. The precursor protein is usually the result of a misfolding event caused by proteolytic cleavage, amino acid substitution, or specific local factors such as β_2-microglobulin. The misfolded proteins are highly prone to self-aggregation into protofilaments and fibrils.[44] Depending on the source of misfolded protein, the most frequent forms are AL amyloidosis, AA amyloidosis, fibrinogen Aa chain amyloidosis, apoliproprotein AI or AII amyloidosis, or hereditary lysozyme amyloidosis. The most important prognostic factors in AA than in AL type amyloidosis are the extent of glomerular, tubulointerstitial and vascular damage.[45] Emerging treatment strategies are based on peptides and small molecules that stabilize precursor proteins and interfere with amyloid protein deposition.[44] One example is serum amyloid P (SAP) that has been radioiodinated for amyloid detection. While SAP binds to all types of amyloid, its specificity for imaging is highest for AA and AL amyloid. Amyloid deposits can also regress by endogenous degradation. Reductions in SAP binding have been attributed to a regression of amyloid deposits.[46] It is also possible that SAP binding represents the formation of new amyloid which may correlate with a deterioration of organ function.

Iodine-131 labeled recombinant beta 2 microglobulin has recently been developed for specific detection of beta 2 microglobulin related amyloidosis in hemodialysis patients.[47] ^{99m}Tc-labeled aprotinin[48] and radioiodinated fibril reactive monoclonal antibodies[49] also provide excellent images of amyloid accumulation.

Functional Consequences of Injury

Until recently, clinical renal imaging focused on the functional consequences of injury. The available tools provide valuable information on organ perfusion, glomerular or tubular function and metabolism. One great advantage of PET imaging is the high organ to background contrast and lack of background activity. Both absolute measurements and split function measurements can be performed with great precision. A further advantage of PET compared with contrast imaging is the subpharmacological dose of the injected tracer hence the lack of allergic reactions or toxic effects.

Glomerular Function

Glomerular filtration has been imaged and quantified in experimental animals using cobalt-55 ethylene diamine tetraacetic acid (EDTA)[50] or gallium-68 EDTA.[51] Gallium-68 has recently been used in an increasing number of works for the radiolabeling of peptides and other macromolecules either directly or by means of a chelator such as DOTA. However, gallium-68 has been used for a very long time for labeling more simple radiopharmaceuticals such as EDTA. Actually, the first $^{68}Ge/^{68}Ga$ generator was eluted by EDTA solution which resulted in chelated gallium-EDTA.[52] Subsequently, a Ga-68 generator was developed that was based on hydroxyquinoline extraction producing Ga-68 oxine at a low breakthrough of Ge-68 of less than 0.003%. The Ga-68 oxine

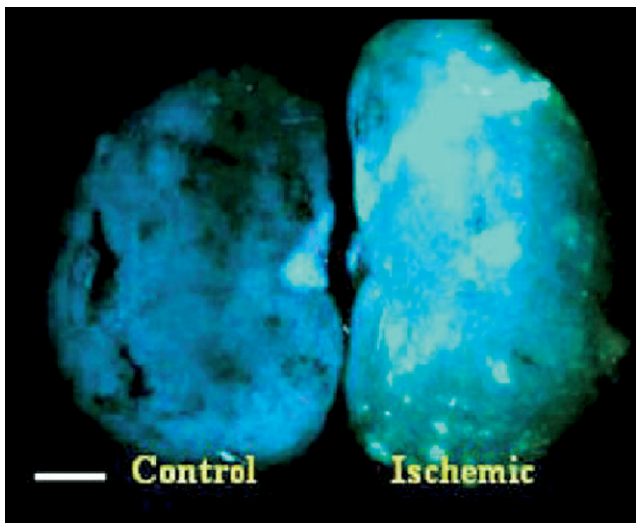

Figure 6 Fluorescent imaging of apoptosis with NST-732 after renal ischemia reperfusion injury. This macroscopic image shows the accumulation in the entire kidney whereas microscopic imaging demonstrated accumulation in tubular cells and correlation with terminal deoxynucleotidyl transferase-mediated dUTP nick end labeling staining.[43] (Reprinted with kind permission from Springer Science and Business Media from Aloya et al.[43]) (Color version of figure is available online.)

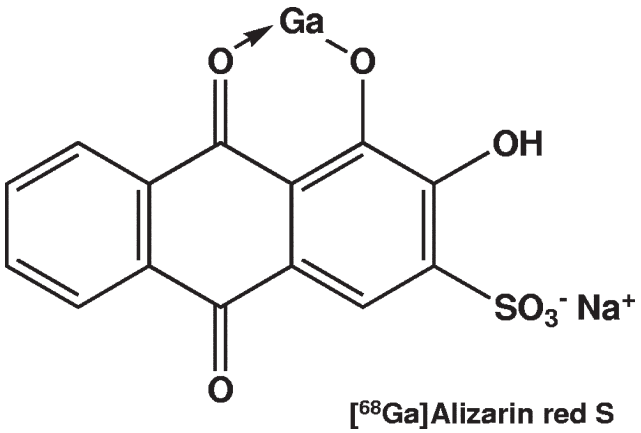

Figure 7 Structure of ^{68}Ga-Alizarin red S.[54]

could be readily converted to other radiopharmaceuticals such as ^{68}Ga-EDTA (renal imaging), ^{68}Ga-EDTMP (bone imaging), or Ga-68 colloid (liver spleen imaging).[53]

Gallium-68 labeled alizarin red S (Fig. 7) is a radiopharmaceutical that is simple to prepare and accumulates in the renal cortex similar to ^{99m}Tc-DMSA. In contrast to DMSA, however, its urinary excretion is low and outstanding cortical accumulation is observed 90 minutes postinjection in human volunteers.[54] This radiopharmaceutical could further improve the diagnosis and assessment of severity of acute pyelonephritis.

Renal Blood Flow

Radiopharmaceuticals used for imaging renal blood flow have a high extraction fraction in the organ. Examples are ^{15}O-water, ^{82}Rb, ^{13}N-ammonia, ^{64}Cu-PTSM,[b] ^{62}Cu-PTSM, and ^{64}Cu-ETS.[c] ^{15}O-water achieves peak activity in the kidneys in the first 30 seconds of a good bolus injection. Because it is a freely diffusible radiopharmaceutical, its tissue concentration curve shows rapid decline after the peak. ^{15}O-water is likely the most physiological substance without any pharmacological effects. It is highly soluble in blood and kidneys and has a blood to kidney partition coefficient of ~1. The disadvantages of ^{15}O-water are that a cyclotron needs to be in the proximity of the PET scanner because of the short half-life of O-15, and for most accurate quantifications, an arterial input function may be required. The statistical noise in the individual scans of a dynamic study may also be substantial.

Rubidium-82 is commercially available for myocardial perfusion imaging in the form of a ^{82}Sr/^{82}Rb generator. The parent isotope strontium-82 has a half-life of 25 days and is absorbed on a hydrous stannic oxide column. Rubidium-82 is eluted with sterile sodium chloride solution from this column. The half-life of Rb-82 is 75 sec and its buildup in the generator is therefore very rapid. Although the radiotoxicity of Rb-82 is low, contaminants with longer half-lives (Sr-82 and Sr-85) can accumulate in the body after repeated injections. The breakthrough of Sr-82 has to be kept under 10^{-5} in proportional radioactivity. Rubidium-82 accumulates over 2 to 3 minutes and follows the kinetics of a trapped radiopharmaceutical due to its slow clearance from the kidney parenchyma.

Radiocopper-labeled radiopharmaceuticals also show high extraction and slow elimination in the kidney. The most important radiopharmaceutical is copper(II)-pyruvaldehyde bis (N-4-methylthiosemicarbazone) (Cu-PTSM) that can be labeled with the positron emitters copper-62 or copper-64. Copper-62 has a half-life of 9.7 minutes and is obtained from a ^{62}Zn/^{62}Cu generator. Copper-64 is a cyclotron product with a half-life of 13 hours. Renal blood flow measured with Cu-PTSM correlates well with the renal blood flow obtained with radioactive microspheres.[55,56]

Nitrogen-13-labeled ammonia has high extraction in the kidneys[57] and has been used in animal models of allograft rejection, unilateral nephrectomy and cyclosporine toxicity.[57,58] Other radiopharmaceuticals that are particularly interesting for quantification of renal blood flow in animal experiments but less likely to achieve clinical acceptance are microspheres radiolabeled with carbon-11[59,60] and Ga-68.[61]

Renal Blood Volume

Determination of organ blood volume is an important research tool that can be incorporated into kinetic models of radiopharmaceuticals to correct tissue activity curves for intravascular activity. Radiolabeled carbon monoxide [^{15}O]CO due to the short half-life of O-15, can only be used when a cyclotron is located near the PET scanner and has to be administered by inhalation.[62-65] Human serum albumin (HSA) has been labeled with copper-62-dithiosemicarbazone (^{62}Cu-HSA-DTS) where copper-62 was obtained from a ^{62}Zn/^{62}Cu generator.[66] Distribution of this radiopharmaceutical will represent the regional plasma rather than blood pool but it can be converted to blood volume after correction for the hematocrit. Organ hematocrit can be determined with the sequential use of ^{62}Cu-HSA-DTS and [^{15}O]CO.[66] Another blood pool imaging agent is gallium-68-DOTA-albumine. Unfortunately, due to the presence of DOTA this radiopharmaceutical is excreted into urine which results in a significant overestimation of renal blood volume.[67]

Metabolism

Carbon-11 labeled acetate has been used for imaging myocardial metabolism but it also appears to be suited for renal imaging. In the kidneys as in the myocardium, both the accumulation and the washout rate of this radiopharmaceutical are important parameters. ^{11}C-acetate has no measurable urinary excretion as the final metabolic product [^{11}C]CO_2 is

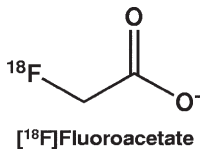

Figure 8 Structure of ^{18}F-Fluoroacetate.[69]

[b]Copper(II)-pyruvaldehyde bis (N-4-methylthiosemicarbazone).
[c]Ethylglyoxal bis(thiosemicarbazone).

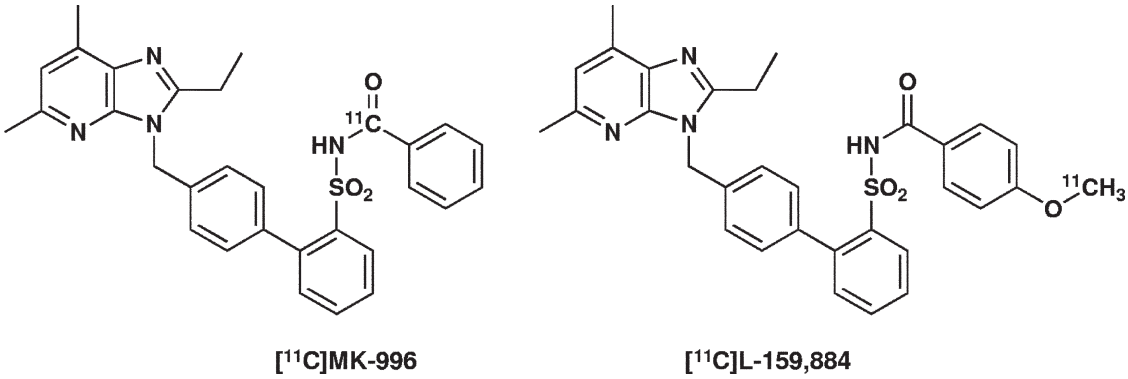

Figure 9 Structures of [11C]MK-996 (left) and [11C]L-159,884 (right).[84]

eliminated from the body by respiration. The uptake of C-11 acetate K1 in the renal tissue is very high at 0.6 to 1.3 and stands for high extraction and the ability to use this tracer for quantification of renal blood flow. In renal artery stenosis, diabetic nephropathy, and hypertensive nephropathy the uptake is significantly reduced.[68]

A derivative of acetate that could be used in routine clinic is ^{18}F-fluoroacetate (Fig. 8). Although fluoroacetate is highly toxic, the radiopharmaceutical mass that would be injected into humans is 1,000,000 times less than the human median lethal dose (LD_{50}).[69] Biodistribution in nonhuman primates has shown excellent accumulation of ^{18}F-fluoroacetate in the kidneys.

Receptors

Angiotensin

Angiotensin II plays a central role in the regulation of renal function. There are 2 angiotensin receptor subtypes in the human body: AT_1R and AT_2R. The AT_1R subtype is highly concentrated in the glomeruli and the medulla and is responsible for most of the functional effects of angiotensin II.[70] In vivo imaging studies with PET performed in dogs showed that the AT_1R was upregulated in estrogen-deficient female animals and in animals on escalating dietary sodium.[71,72] These findings may help elucidate the sodium sensitivity observed in men and aged women.[73] The AT_2R is mostly active during embryonal development and is much less expressed in the adult kidney.

Angiotensin receptor blockers (ARBs) with high affinity and selectivity for the AT1R have been radiolabeled for PET imaging. The first generation of these radioligands includes MK-996 (L-159,282) and L-159,884 (Fig. 9). Of these two related ligands, [11C]L-159,884 has the more favorable biodistribution, including a lack of urinary excretion; consequently, it has been used in most PET experiments published so far.[71,72,74-81]

KR31173 (Fig. 10) is a derivative of the potent AT_1R antagonist SK-1080[82,83] that has been radiolabeled using ^{11}C-methyl iodide.[84] Biodistribution in mice showed high specific uptake of ^{11}C-KR31173 in the adrenal glands and kidneys with tissue-to-blood ratios greater than 10. AT1R subtype selectivity was confirmed by pretreatment of the animals with the AT_2R antagonist PD123,319. High accumulation and specific binding in the baboon kidney[85] make ^{11}C-KR31173 a promising radiopharmaceutical for human studies.

Angiotensin II concentrations within the kidney are 1,000-fold higher than in the circulation, which is consistent with the existence of a local, intrarenal renin-angiotensin system.[86] The kidneys, like many other organs, possess the ability to synthesize angiotensinogen and convert it to angiotensin II via angiotensin I. The regulation of these steps is very important physiologically and alterations of any of these regulatory steps can be involved in diseases. The angiotensin-

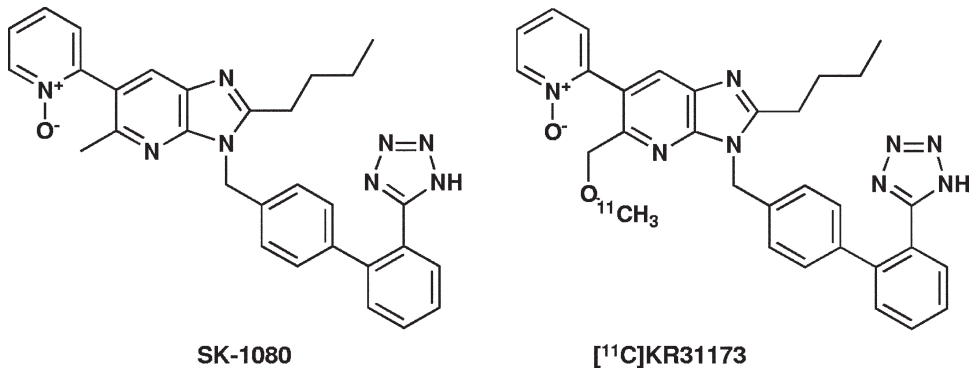

Figure 10 Structures of SK-1080 (left) and ^{11}C-KR31173 (right).[84]

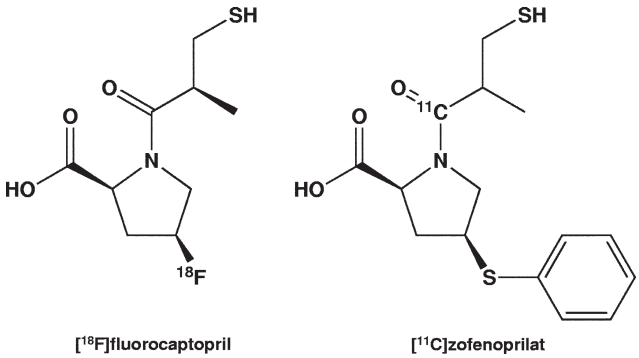

Figrue 11 Radiolabeled ACE inhibitors: ^{18}F-Fluorocaptopril (left) and ^{11}C-zofenoprilat (right).[88,90]

converting enzyme (ACE) is an important target for treatment of hypertension and was one of the first renal molecular targets explored for imaging. The reason for this is that at present no drugs, other than antibodies are available that bind to angiotensin, angiotensin I or angiotensin II.

Sulfydryl (example: captopril), carboxyl (example: enalapril), and phosphorus containing (example: fosinopril) compounds are 3 classes of ACE inhibitors based on their zinc binding moieties.[87] Two of the sulfydryl containing drugs have been radiolabeled for PET: ^{18}F-Fluorocaptopril and ^{11}C-zofenoprilat (Fig. 11).

Fluorocaptopril was synthesized by nucleophilic substitution of a triflate precursor.[88] Biodistribution showed high accumulation in the lungs, kidney, and aortic wall and the specific binding was 86% in the kidneys. PET studies in humans showed that accumulation and specific binding was also high in both lungs and kidney with a tighter binding to the kidneys. Clinical studies showed reduced pulmonary ACE in primary pulmonary hypertension.[89]

Zofenopril is an ACE inhibitor with a four times higher potency than captopril.[87] The bioactive metabolite ^{11}C-zofenoprilat was synthesized by acylation of (*S*)-4-phenylthio-L-proline methyl ester with ^{11}C-methacryloyl chloride followed by a Michael addition with thiobenzoic acid.[90] In a human subject, distinct organ accumulation with organ-to-blood ratios greater than 1 was seen in the liver, kidney, and

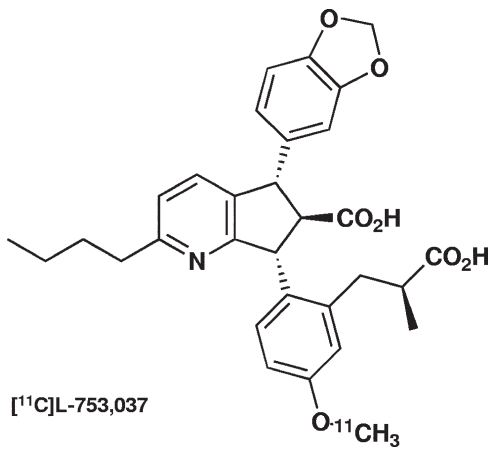

Figure 12 Structure of ^{11}C-L-753,037.[96]

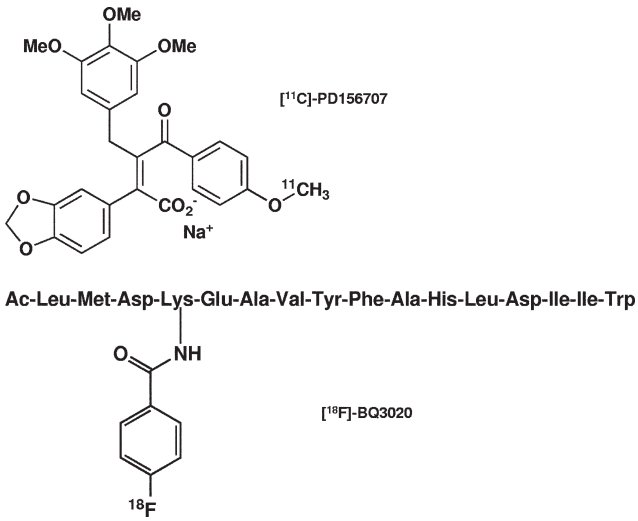

Figure 13 Structures of ^{11}C-PD156707 (upper) and ^{18}F-BQ3020 (lower).[97,98]

lungs. Accumulation in the gall bladder indicated hepatobiliary excretion.[90] First studies were performed with a diastereometric mixture. Improved specific binding is expected with stereospecific labeling of the (S,S,S) isoform that has 156 times higher pharmacological potency than the (R,S,S) isoform.[90]

Endothelin

Endothelins (ETs) are tissue hormones that cause vasoconstriction, decreased renal blood flow and reduced glomerular filtration. ETs share a marked structural similarity to the sarafotoxins, peptides isolated from the Israeli burrowing asp (*Atractaspis engaddensis*).[91] Of the 3 peptides ET-1, ET-2, and ET-3, it is ET-1 that has the greatest significance for both physiology and pathology. There are 2 endothelin receptor subtypes, ETAR and ETBR. In the kidneys, ETAR is expressed in the renal arteries and afferent and efferent glomerular arterioles while ETBR is expressed by the endothelium of glomeruli and vasa recta. Expression of endothelin receptors in the tubular epithelium is low.

Renal release of ET-1 is increased in ischemic acute renal failure, transplant rejection, essential hypertension and

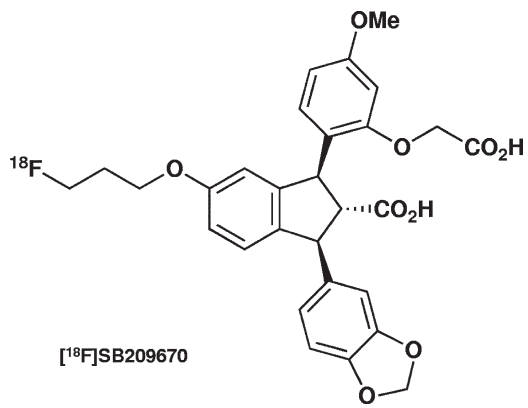

Figure 14 Structure of ^{18}F-SB209670.[100]

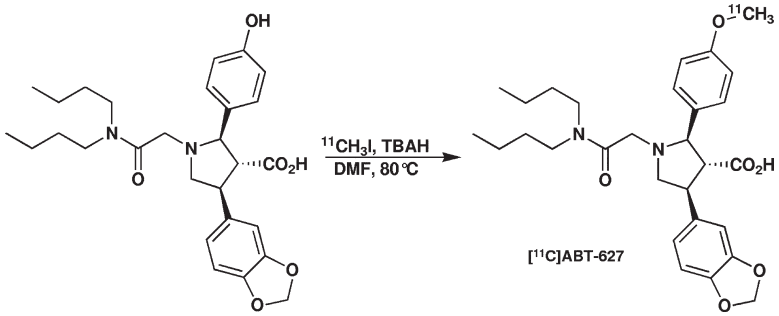

Figure 15 Radiosynthesis of the ETA selective antagonist [^{11}C]ABT-627.[101]

chronic renal failure. ET-1 is involved in the pathogenesis of proliferative glomerulonephritis with significant upregulation of ETAR in the proximal and distal tubules.[91] The ETAR is upregulated in experimental diabetes; ET-1 as well as ETAR are probably involved in the process of vasoconstriction, mesangial mitogenesis and endothelial proliferation of diabetic nephropathy.[92]

The nonselective agonist peptide endothelin-1 has been labeled with both radioiodine[93] and fluorine-18.[94] A nonselective antagonist for endothelin receptor imaging is [^{11}C]L-753,037 (Fig. 12). It has been synthesized by carbon-11 methylation of the corresponding phenolic precursor.[95] Ex vivo studies in mice using [^{11}C]L-753,037 showed uptake in the liver, adrenals, kidneys, heart, and lungs,[96] organs known to express high concentrations of endothelin receptors.[93] The uptake of [^{11}C]L-753,037 was displaced by both ETAR selective and nonselective blocking drugs. In vivo PET imaging in a dog showed similar results.[94]

The first selective PET radioligands were the ETA selective antagonist ^{11}C-PD156707 and the ETB selective agonist ^{18}F-BQ3020 (Fig. 13).[97,98] The specific activity of ^{11}C-PD156707, however, was low and this radioligand has not been used for in vivo imaging. ETA selective radioligands with improved binding characteristics have been synthesized,[99-101] but thus far, none have been used for imaging ET receptors in humans.

The radiopharmaceutical ^{18}F-SB209670 (Fig. 14) has selective binding to the ETAR receptor with subnanomolar affinity. It has been synthesized from its precursor by alkylation with ^{18}F-fluoropropylbromide. This radiopharmaceutical demonstrated high accumulation in the kidneys.[100]

ABT-627 is an ETAR selective drug that has been radiolabeled by ^{11}C-methylation (Fig. 15) of its desmethyl precursor. Biodistribution in mice showed accumulation in liver and kidneys but not in the myocardium. A PET study in a baboon showed 50% specific binding in the myocardium.[101]

The selective ETBR agonist ^{18}F-BQ3020 was labeled in the ε-amino group of Lys^9 by conjugation with *N*-succinimidyl 4-[^{18}F]fluorobenzoate. In vitro binding to human kidney tissue was inhibited by ET-1 and unlabeled BQ3020 but not by ETAR selective antagonists, signifying the selectivity of ^{18}F-BQ3020 for the ETBR. MicroPET imaging showed accumulation of ^{18}F-BQ3020 in rabbit kidney with higher activity in the medulla than renal cortex.[98]

Closing Remarks

The high spatial resolution, high detecting sensitivity, and quantitative accuracy of PET make this imaging modality ideal for development of novel molecular techniques to serve as sensitive biomarkers of renal injury. To develop radiopharmaceuticals for molecular imaging of the kidneys, one has to keep in mind the specifics of renal anatomy and function and factors related to the molecular pathology of the kidneys.

Image registration, image fusion and to a certain degree, partial volume correction can better be achieved if anatomical information is obtained in the same session. Although it may not be possible to separately image the glomeruli or the juxtaglomerular apparatus, some molecular targets are highly concentrated in these structures and will dominate the PET signal. It is also important to understand the functional implications pathogenetic mechanisms linked to the modulation of specific target molecules and their sensitivity and specificity for renal pathologies.

The distribution and kinetics of any radiopharmaceutical may be influenced by renal blood flow, glomerular filtration, tubular extraction, and tubular excretion. An ideal radiopharmaceutical for imaging renal blood flow is one with high extraction in the kidneys and slow washout into the tubular lumen or back into circulation. An ideal radiopharmaceutical for imaging glomerular function will be one with low plasma protein binding, high glomerular extraction and no tubular accumulation. Cortical imaging is best achieved with a radiopharmaceutical that has high extraction and slow clearance in the tubular epithelium but no accumulation in the collecting system. For virtually any radiopharmaceutical, it is advantageous if it is not metabolized and if its protein binding is low.

As far as the molecular pathology is concerned, the best targets are those that are upregulated in renal injury. Specificity for acuteness or chronicity may be desirable although this can be supplemented by clinical history and physical examination. Similarly, for certain pathologies, selective expression only in the pathology of interest can be an advantage if the disease has high prevalence. Otherwise, development of sensitive but less specific radiopharmaceuticals could be the goal.

References

1. Toronyi E, Hamar J, Magyar K, et al: Antiapoptotic effect of (-)-deprenyl in rat kidney after ischemia-reperfusion. Med Sci Monit 8:BR65-BR68, 2002
2. Haller H, Maasch C, Dragun D, et al: Antisense oligodesoxynucleotide strategies in renal and cardiovascular disease. Kidney Int 53:1550-1558, 1998
3. Logan J, Fowler JS, Volkow ND, et al: Reproducibility of repeated measures of deuterium substituted [11C]L-deprenyl ([11C]L-deprenyl-D2) binding in the human brain. Nucl Med Biol 27:43-49, 2000
4. Feinendegen LE, Herzog H, Wieler H, et al: Glucose transport and utilization in the human brain: Model using carbon-11 methylglucose and positron emission tomography. J Nucl Med 27:1867-1877, 1986
5. Tian X, Chakrabarti A, Amirkhanov N, et al: Receptor-mediated internalization of chelator-PNA-peptide hybridization probes for radioimaging or magnetic resonance imaging of oncogene mRNAs in tumours. Biochem Soc Trans 35:72-76, 2007
6. Tian X, Chakrabarti A, Amirkhanov NV, et al: External imaging of CCND1, MYC, and KRAS oncogene mRNAs with tumor-targeted radionuclide-PNA-peptide chimeras Ann N Y Acad Sci 1059:106-144, 2005
7. Redaelli CA, Tien YH, Kubulus D, et al: Hyperthermia preconditioning induces renal heat shock protein expression, improves cold ischemia tolerance, kidney graft function and survival in rats. Nephron 90:489-497, 2002
8. Eckardt KU, Bernhardt WM, Weidemann A, et al: Role of hypoxia in the pathogenesis of renal disease. Kidney Int Suppl S46-S51, 2005
9. Blantz RC, Thomson SC, Peterson OW, et al: Physiologic adaptations of the tubuloglomerular feedback system [review]. Kidney Int 38:577-583, 1990
10. Schnermann J, Briggs JP: Effect of angiotensin and other pressor agents on tubuloglomerular feedback responses. Kidney Int Suppl 30:S77-S80, 1990
11. Cervenka L, Kramer HJ, Maly J, et al: Role of nNOS in regulation of renal function in angiotensin II-induced hypertension. Hypertension 38:280-285, 2001
12. Braam B, Navar LG, Mitchell KD: Modulation of tubuloglomerular feedback by angiotensin II type 1 receptors during the development of Goldblatt hypertension. Hypertension 25:1232-1237, 1995
13. Anderson WP, Kett MM, Stevenson KM, et al: Renovascular hypertension: Structural changes in the renal vasculature. Hypertension 36: 648-652, 2000
14. Denton KM, Anderson WP, Sinniah R: Effects of angiotensin II on regional afferent and efferent arteriole dimensions and the glomerular pole. Am J Physiol Regul Integr Comp Physiol 279:R629-R638, 2000
15. Denton KM, Fennessy PA, Alcorn D, et al: Morphometric analysis of the actions of angiotensin II on renal arterioles and glomeruli. Am J Physiol 262:F367-F372, 1992
16. Simon M, Rockl W, Hornig C, et al: Receptors of vascular endothelial growth factor/vascular permeability factor (VEGF/VPF) in fetal and adult human kidney: Localization and [125I]VEGF binding sites. J Am Soc Nephrol 9:1032-1044, 1998
17. Kanellis J, Paizis K, Cox AJ, et al: Renal ischemia-reperfusion increases endothelial VEGFR-2 without increasing VEGF or VEGFR-1 expression. Kidney Int 61:1696-1706, 2002
18. Rini BI, Rathmell WK: Biological aspects and binding strategies of vascular endothelial growth factor in renal cell carcinoma. Clin Cancer Res 13:741s-746s, 2007
19. Hainsworth JD, Sosman JA, Spigel DR, et al: Treatment of metastatic renal cell carcinoma with a combination of bevacizumab and erlotinib. J Clin Oncol 23:7889-7896, 2005
20. Nagengast WB, de Vries EG, Hospers GA, et al: In Vivo VEGF imaging with radiolabeled bevacizumab in a human ovarian tumor xenograft. J Nucl Med 48:1313-1319, 2007
21. Cooper ME, Vranes D, Youssef S, et al: Increased renal expression of vascular endothelial growth factor (VEGF) and its receptor VEGFR-2 in experimental diabetes. Diabetes 48:2229-2239, 1999
22. Cai W, Chen K, Mohamedali KA, et al: PET of vascular endothelial growth factor receptor expression. J Nucl Med 47:2048-2056, 2006
23. Aiello LP, Pierce EA, Foley ED, et al: Suppression of retinal neovascularization in vivo by inhibition of vascular endothelial growth factor (VEGF) using soluble VEGF-receptor chimeric proteins. Proc Natl Acad Sci USA 92:10457-10461, 1995
24. Robinson GS, Pierce EA, Rook SL, et al: Oligodeoxynucleotides inhibit retinal neovascularization in a murine model of proliferative retinopathy. Proc Natl Acad Sci USA 93:4851-4856, 1996
25. Ostendorf T, De Vriese AS, Floege J: Renal side effects of anti-VEGF therapy in man: A new test system. Nephrol Dial Transplant 22:2778-2780, 2007
26. Otani A, Takagi H, Suzuma K, et al: Angiotensin II potentiates vascular endothelial growth factor-induced angiogenic activity in retinal microcapillary endothelial cells. Circ Res 82:619-628, 1998
27. Moravski CJ, Kelly DJ, Cooper ME, et al: Retinal neovascularization is prevented by blockade of the renin-angiotensin system. Hypertension 36:1099-1104, 2000
28. Collingridge DR, Carroll VA, Glaser M, et al: The development of [(124)I]iodinated-VG76e: A novel tracer for imaging vascular endothelial growth factor in vivo using positron emission tomography. Cancer Res 62:5912-5919, 2002
29. Cai W, Chen X: Multimodality imaging of vascular endothelial growth factor and vascular endothelial growth factor receptor expression. Front Biosci 12:4267-4279, 2007
30. Choe YS, Lee KH: Targeted in vivo imaging of angiogenesis: present status and perspectives. Curr Pharm Des 13:17-31, 2007
31. Haubner R, Wester HJ, Weber WA, et al: Noninvasive imaging of alpha(v) beta3 integrin expression using 18F-labeled RGD-containing glycopeptide and positron emission tomography. Cancer Res 61: 1781-1785, 2001
32. Haubner R, Weber WA, Beer AJ, et al: Noninvasive visualization of the activated alphavbeta3 integrin in cancer patients by positron emission tomography and [18F]Galacto-RGD. PLoS Med 2:e70, 2005
33. Chen X, Sievers E, Hou Y, et al: Integrin alpha v beta 3-targeted imaging of lung cancer. Neoplasia 7:271-279, 2005
34. Yang DJ, Kim KD, Schechter NR, et al: Assessment of antiangiogenic effect using 99mTc-EC-endostatin. Cancer Biother Radiopharm 17: 233-245, 2002
35. Lee KH, Song SH, Paik JY, et al: Specific endothelial binding and tumor uptake of radiolabeled angiostatin. Eur J Nucl Med Mol Imaging 30:1032-1037, 2003
36. Shiue CY, Shiue GG, Alavi AA, et al: [^{18}F]Fluoropropylsqualamine as an angiogenesis imaging agent. J Labelled Compounds Radiopharmaceuticals 44:S391-S392, 2001
37. Mene P, Amore A: Apoptosis: potential role in renal diseases. Nephrol Dial Transplant 13:1936-1943, 1998
38. Gobe GC, Harmon B, Leighton J, et al: Radiation-induced apoptosis and gene expression in neonatal kidney and testis with and without protein synthesis inhibition. Int J Radiat Biol 75:973-983, 1999
39. Murakami Y, Takamatsu H, Taki J, et al: 18F-labelled annexin V: A PET tracer for apoptosis imaging. Eur J Nucl Med Mol Imaging 31: 469-474, 2004
40. Keen HG, Dekker BA, Disley L, et al: Imaging apoptosis in vivo using 124I-annexin V and PET. Nucl Med Biol 32:395-402, 2005
41. Bauer C, Bauder-Wuest U, Mier W, et al: 131I-Labeled peptides as caspase substrates for apoptosis imaging. J Nucl Med 46:1066-1074, 2005
42. Cauchon N, Langlois R, Rousseau JA, et al: PET imaging of apoptosis with (64)Cu-labeled streptavidin following pretargeting of phosphatidylserine with biotinylated annexin-V. Eur J Nucl Med Mol Imaging 34:247-258, 2007
43. Aloya R, Shirvan A, Grimberg H, et al: Molecular imaging of cell death in vivo by a novel small molecule probe. Apoptosis 11:2089-2101, 2006
44. Dember LM: Amyloidosis-associated kidney disease. J Am Soc Nephrol 17:3458-3471, 2006
45. Sasatomi Y, Sato H, Chiba Y, et al: Prognostic factors for renal amyloidosis: A clinicopathological study using cluster analysis. Intern Med 46:213-219, 2007

46. Hawkins PN: Studies with radiolabelled serum amyloid P component provide evidence for turnover and regression of amyloid deposits in vivo. Clin Sci (Lond) 87:289-295, 1994
47. Schaffer J, Burchert W, Floege J, et al: Recombinant versus natural human 111In-beta2-microglobulin for scintigraphic detection of Abeta2m amyloid in dialysis patients. Kidney Int 58:873-880, 2000
48. Schaadt BK, Hendel HW, Gimsing P, et al: 99mTc-aprotinin scintigraphy in amyloidosis. J Nucl Med 44:177-183, 2003
49. Wall JS, Kennel SJ, Paulus M, et al: Radioimaging of light chain amyloid with a fibril-reactive monoclonal antibody. J Nucl Med 47:2016-2024, 2006
50. Goethals P, Volkaert A, Vandewielle C, et al: 55Co-EDTA for renal imaging using positron emission tomography (PET): A feasibility study. Nucl Med Biol 27:77-81, 2000
51. Yamashita M, Inaba T, Kawase Y, et al: Quantitative measurement of renal function using Ga-68-EDTA. Tohoku J Exp Med 155:207-208, 1988
52. Greene MW, Tucker WD: An improved gallium-68 cow. Int J Appl Radiat Isot 12:62-63, 1961
53. Ehrhardt GJ, Welch MJ: A new germanium-63/gallium-68 generator. J Nucl Med 19:925-929, 1978
54. Schuhmacher J, Maier-Borst W, Wellman HN: Liver and kidney imaging with Ga-68-labeled dihydroxyanthraquinones. J Nucl Med 21: 983-987, 1980
55. Young H, Carnochan P, Zweit J, et al: Evaluation of copper(II)-pyruvaldehyde bis (N-4-methylthiosemicarbazone) for tissue blood flow measurement using a trapped tracer model. Eur J Nucl Med 21:336-341, 1994
56. Shelton ME, Green MA, Mathias CJ, et al: Assessment of regional myocardial and renal blood flow with copper-PTSM and positron emission tomography. Circulation 82:990-997, 1990
57. Nitzsche EU, Choi Y, Killion D, et al: Quantification and parametric imaging of renal cortical blood flow in vivo based on Patlak graphical analysis. Kidney Int 44:985-996, 1993
58. Killion D, Nitzsche E, Choi Y, et al: Positron emission tomography: A new method for determination of renal function. J Urology 150:1064-1068, 1993
59. Brooks DJ, Frackowiak RS, Lammertsma AA, et al: A comparison between regional cerebral blood flow measurements obtained in human subjects using 11C-methylalbumin microspheres, the C15O2 steady-state method, and positron emission tomography. Acta Neurol Scand 73:415-422, 1986
60. Turton DR, Brady F, Pike VW, et al: Preparation of human serum [methyl-11C]methylalbumin microspheres and human serum [methyl-11C]methylalbumin for clinical use. Int J Appl Radiation and Isotopes 35:337-344, 1984
61. Mintun MA, Ter Pogossian MM, Green MA, et al: Quantitative measurement of regional pulmonary blood flow with positron emission tomography. J Appl Physiol 60:317-326, 1986
62. Hermansen F, Ashburner J, Spinks TJ, et al: Generation of myocardial factor images directly from the dynamic oxygen-15-water scan without use of an oxygen-15-carbon monoxide blood-pool scan. J Nucl Med 39:1696-1702, 1998
63. Kubo T, Kimori K, Nakamura F, et al: Blood flow and blood volume in the femoral heads of healthy adults according to age: measurement with positron emission tomography (PET). Ann Nucl Med 15:231-235, 2001
64. Kihlberg T, Karimi F, Langstrom B: [(11)C] Carbon monoxide in selenium-mediated synthesis of (11)C-carbamoyl compounds. J Org Chem 67:3687-3692, 2002
65. Hofman HA, Knaapen P, Boellaard R, et al: Measurement of left ventricular volumes and function with O-15-labeled carbon monoxide gated positron emission tomography: comparison with magnetic resonance imaging. J Nucl Cardiol 12:639-644, 2005
66. Okazawa H, Yonekura Y, Fujibayashi Y, et al: Measurement of regional cerebral plasma pool and hematocrit with copper-62-labeled HSA-DTS. J Nucl Med 37:1080-1085, 1996
67. Hoffend J, Mier W, Schuhmacher J, et al: Gallium-68-DOTA-albumin as a PET blood-pool marker: experimental evaluation in vivo. Nucl Med Biol 32:287-292, 2005
68. Shreve P, Chiao PC, Humes HD, et al: Carbon-11-acetate PET imaging in renal disease. J Nucl Med 36:1595-1601, 1995
69. Ponde DE, Dence CS, Oyama N, et al: 18F-fluoroacetate: A potential acetate analog for prostate tumor imaging—in vivo evaluation of 18F-fluoroacetate versus 11C-acetate. J Nucl Med 48:420-428, 2007
70. Johnson HA: Diagnosis by the bit: A method for evaluating the diagnostic process. Ann Clin Lab Sci 19:323-331, 1989
71. Szabo Z, Speth RC, Brown PR, et al: Use of positron emission tomography to study AT1 receptor regulation in vivo. J Am Soc Nephrol 12:1350-1358, 2001
72. Owonikoko TK, Fabucci ME, Brown PR, et al: In vivo investigation of estrogen regulation of adrenal and renal angiotensin AT1 receptor expression by PET. J Nucl Med 45:94-100, 2003
73. Weinberger MH, Fineberg NS, Fineberg SE, et al: Salt sensitivity, pulse pressure, and death in normal and hypertensive humans. Hypertension 37:429-432, 2001
74. Szabo Z, Mathews WB, Burns HD, Gibson RE, Kivlighn SD, Hamill TG, Ravert HT, Dannals RF. Comparison of the pharmacological potency and AT1 receptor occupancy of the nonpeptide angiotensin antagonist E-3174. J Nucl Med 37:288P, 1996
75. Kao PF, Szabo Z, Dannals RF, et al: Compartmental modeling of an angiotensin IP/AT1 receptor imaging agent: C-11 L-159,884. J Nucl Med 35:137P, 1994
76. Kao PF, Szabo Z, Dannals RF, et al: Impulse response function of the angiotensin II/AT1 receptor imaging agent: Carbon-11 L-159,884. Eur J Nucl Med 21:774, 1994 (suppl)
77. Kim SE, Scheffel U, Szabo Z, et al: In vivo labeling of angiotensin II receptors with a carbon-11-labeled selective nonpeptide antagonist. J Nucl Med 37:307-311, 1996
78. Szabo Z, Sandberg K, Brown P, et al: Increased AT1 receptor expression after treatment with the ACE inhibitor lisinopril. J Nucl Med 40:92P-93P, 1999
79. Szabo Z, Kao PF, Burns HD, et al: Investigation of angiotensin II/AT1 receptors with carbon-11-L-159,884: a selective AT1 antagonist. J Nucl Med 39:1209-1213, 1998
80. Zober TG, Brown RP, Sandberg K, et al: PET demonstrates upregulation of the renal angiotensin-II (AT1) receptors in experimental renovascular hypertension. J Nucl Med 44:142P, 2003
81. Szabo Z, Kao PF, Mathews WB, et al: Validation of the impulse response function of [C-11]L-159,884, an angiotensin II, AT1 selective tracer. J Nucl Med 37:288P, 1996
82. Hong KW, Kim CD, Lee SH, et al: The in vitro pharmacological profile of KR31080, a nonpeptide AT1 receptor antagonist. Fundam Clin Pharmacol 12:64-69, 1998
83. Lee BH, Seo HW, Kwon KJ, et al: In vivo pharmacologic profile of SK-1080, an orally active nonpeptide AT1-receptor antagonist. J Cardiovasc Pharmacol 33:375-382, 1999
84. Mathews WB, Yoo SE, Lee SH, et al: A novel radioligand for imaging the AT1 angiotensin receptor with PET. Nucl Med Biol 31:571-574, 2004
85. Zober TG, Seckin E, Mathews WB, et al: Imaging the AT1 receptor with the radioligand [^{11}C]KR31173 and PET in mice, dogs and baboons. Nucl Med Biol 33:5-13, 2006
86. Kim S, Iwao H: Molecular and cellular mechanisms of angiotensin II-mediated cardiovascular and renal diseases. Pharmacol Rev 52:11-34, 2000
87. Unger T, Gohlke P: Converting enzyme inhibitors in cardiovascular therapy: current status and future potential. Cardiovasc Res 28:146-158, 1994
88. Hwang DR, Eckelman WC, Mathias CJ, et al: Positron-labeled angiotensin-converting enzyme (ACE) inhibitor: fluorine-18-fluorocaptopril. Probing the ACE activity in vivo by positron emission tomography. J Nucl Med 32:1730-1737, 1991
89. Qing F, McCarthy TJ, Markham J, et al: Pulmonary angiotensin-converting enzyme (ACE) binding and inhibition in humans. A positron emission tomography study. Am J Respir Crit Care Med 161:2019-2025, 2000

90. Matarrese M, Salimbeni A, Turolla EA, et al: 11C-Radiosynthesis and preliminary human evaluation of the disposition of the ACE inhibitor [11C]zofenoprilat. Bioorg Med Chem 12:603-611, 2004
91. Naicker S, Bhoola KD: Endothelins: Vasoactive modulators of renal function in health and disease. Pharmacol Ther 90:61-88, 2001
92. Khan MA, Dashwood MR, Mumtaz FH, et al: Upregulation of endothelin A receptor sites in the rabbit diabetic kidney: potential relevance to the early pathogenesis of diabetic nephropathy. Nephron 83:261-267, 1999
93. Gibson RE, Fioravanti C, Francis B, et al: Radioiodinated endothelin-1: A radiotracer for imaging endothelin receptor distribution and occupancy. Nucl Med Biol 26:193-199, 1999
94. Johnstrom P, Harris NG, Fryer TD, et al: (18)F-Endothelin-1, a positron emission tomography (PET) radioligand for the endothelin receptor system: Radiosynthesis and in vivo imaging using microPET. Clin Sci (Lond) 103 Suppl 48:4S-8S, 2002
95. Ravert HT, Mathews WB, Hamill TG, et al: Radiosynthesis of a potent endothelin receptor antagonist. J Label Compounds Radiopharm 43: 1205-1210, 2000
96. Aleksic S, Szabo Z, Scheffel U, et al: In vivo labeling of endothelin receptors with [^{11}C]L-753,037: Studies in mice and a dog. J Nucl Med 42:1274-1280, 2001
97. Johnstrom P, Aigbirhio FI, Clark JC, et al: Syntheses of the first endothelin-A- and -B-selective radioligands for positron emission tomography. J Cardiovasc Pharmacol 36:S58-S60, 2000
98. Johnstrom P, Rudd JH, Richards HK, et al: Imaging endothelin ET(B) receptors using [18F]-BQ3020: In vitro characterization and positron emission tomography (microPET). Exp Biol Med (Maywood) 231: 736-740, 2006
99. Hoeltke C, Wagner S, Breyholz HJ, et al: Development, synthesis and in vitro evaluation of novel ET-A receptor PET-radioligands based on PD 156707. J Label Compds Radiopharm 50:S345, 2007
100. Johnstrom P, Fryer TD, Richards HK, et al: In vivo imaging of cardiovascular endothelin receptors using the novel radiolabelled antagonist [18F]-SB209670 and positron emission tomography (microPET). J Cardiovasc Pharmacol 44:S34-S38, 2004
101. Mathews WB, Zober TG, Ravert HT, et al: Synthesis and in vivo evaluation of a PET radioligand for imaging the endothelin-A receptor. Nucl Med Biol 33:15-19, 2006